Cureus

Open Access Original Article

DOI: 10.7759/cureus.218

The Mathematics of Three or More N-Localizers for Stereotactic Neurosurgery

Russell A. Brown [1]

1. Principal Engineer, A9.com

Corresponding author: Russell A. Brown, russ.brown@yahoo.com

Disclosures can be found in Additional Information at the end of the article

Abstract

The mathematics that were originally developed for the N-localizer apply to three N-localizers that produce three sets of fiducials in a tomographic image. Some applications of the N-localizer use four N-localizers; however, the mathematics that apply to three N-localizers do not apply to four N-localizers. One solution to this problem is to ignore one of the four N-localizers in order that the mathematics that apply to three N-localizers may be used. This article presents a novel solution that applies to three or more N-localizers without the requirement that any N-localizer be ignored. This solution provides a transformation matrix that transforms coordinates from the two-dimensional coordinate system of a tomographic image into the three-dimensional coordinate system of the stereotactic frame. In addition, this solution provides a statistical measure of the accuracy of the transformation that may be influenced by conditions, such as nonlinear distortion of the tomographic image.

Categories: Medical Physics, Radiation Oncology, Neurosurgery
Keywords: stereotactic neurosurgery, stereotactic radiosurgery, magnetic resonance imaging, computed tomography, n-localizer

Introduction

Following its invention at the University of Utah in 1978 [1,2], the N-localizer (Figure *1*) was presented at neurosurgery conferences in America and Europe [1, 3]. Beginning in 1979, it was adopted by six different stereotactic frames to enable image-guided surgery and radiosurgery in conjunction with computed tomography (CT), magnetic resonance (MR), and positron emission tomography (PET) [4-41]. Regarding these six stereotactic frames, the Riechert-Mundinger frame that was adapted to CT at Duke University [9, 16] and the Pfizer frame that was constructed in collaboration with the Univeristy of Pittsburgh [5, 10, 27] were used at only those institutions. The Kelly-Goerss [8, 12] frame was the first to be adapted to PET [32]. The Brown-Roberts-Wells (BRW) [4, 7, 13, 15], Leksell [6, 14, 18], and Cosman-Roberts-Wells (CRW) [26, 29] frames achieved widespread use throughout the world.

Received 09/07/2014
Review began 09/15/2014
Review ended 10/11/2014
Published 10/12/2014

How to cite this article
Brown R A (October 12, 2014) The Mathematics of Three or More N-Localizers for Stereotactic Neurosurgery. Cureus 6(10): e218. DOI 10.7759/cureus.218

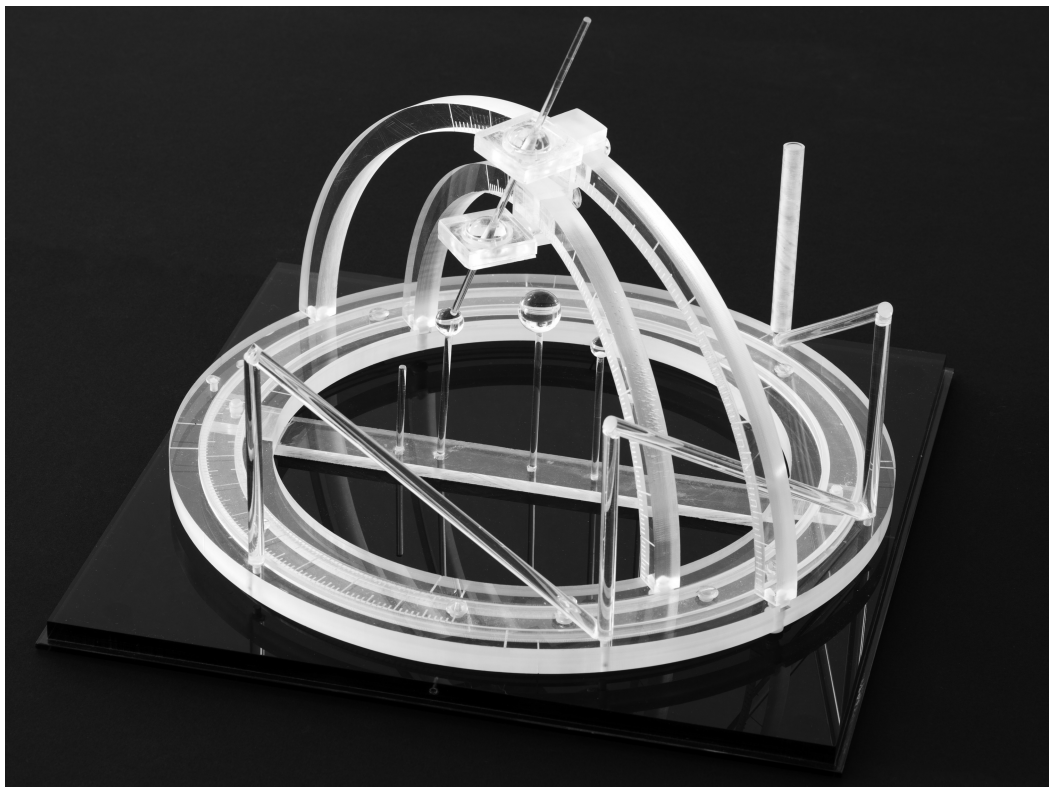

FIGURE 1: Three N-localizers attached to a stereotactic frame

This stereotactic frame was constructed by the author in August 1978 in order to test the concept of the N-localizer. It was presented to the Western Neurological Society and the American Academy of Neurological Surgery in October 1978 [1] and at the 12th INSERM Symposium on Stereotactic Irradiations in July 1979 [3]. Three N-localizers are attached to this frame and are merged end-to-end such that only seven rods are required for image guidance.

Recent review articles discuss the origin and mathematics of the N-localizer [42-45]. The mathematics are summarized in the remainder of this Introduction in preparation for the presentation of new developments in the Materials & Methods section of this article. The reader who is already familiar with the mathematics of the N-localizer may choose to skip directly to the Materials & Methods section.

The N-localizer comprises a diagonal rod that extends from the top of one vertical rod to the bottom of another vertical rod (Figure *2*). In the tomographic image, the cross section of each of the two vertical rods creates a fiducial circle and the cross section of the diagonal rod creates a fiducial ellipse. The ellipse moves away from one circle and towards the other circle as the position of the tomographic section moves downward with respect to the N-localizer. The relative spacing between these three fiducials permits precise localization of the tomographic section relative to the N-localizer. The distance d_{AB} between the centers of circle A and ellipse B and the distance d_{AC} between the centers of circles A and C are used to calculate the ratio $f = d_{AB}/d_{AC}$. This ratio represents the fraction of diagonal rod B that extends from the top of vertical rod A to the point of intersection of rod B with the tomographic section.

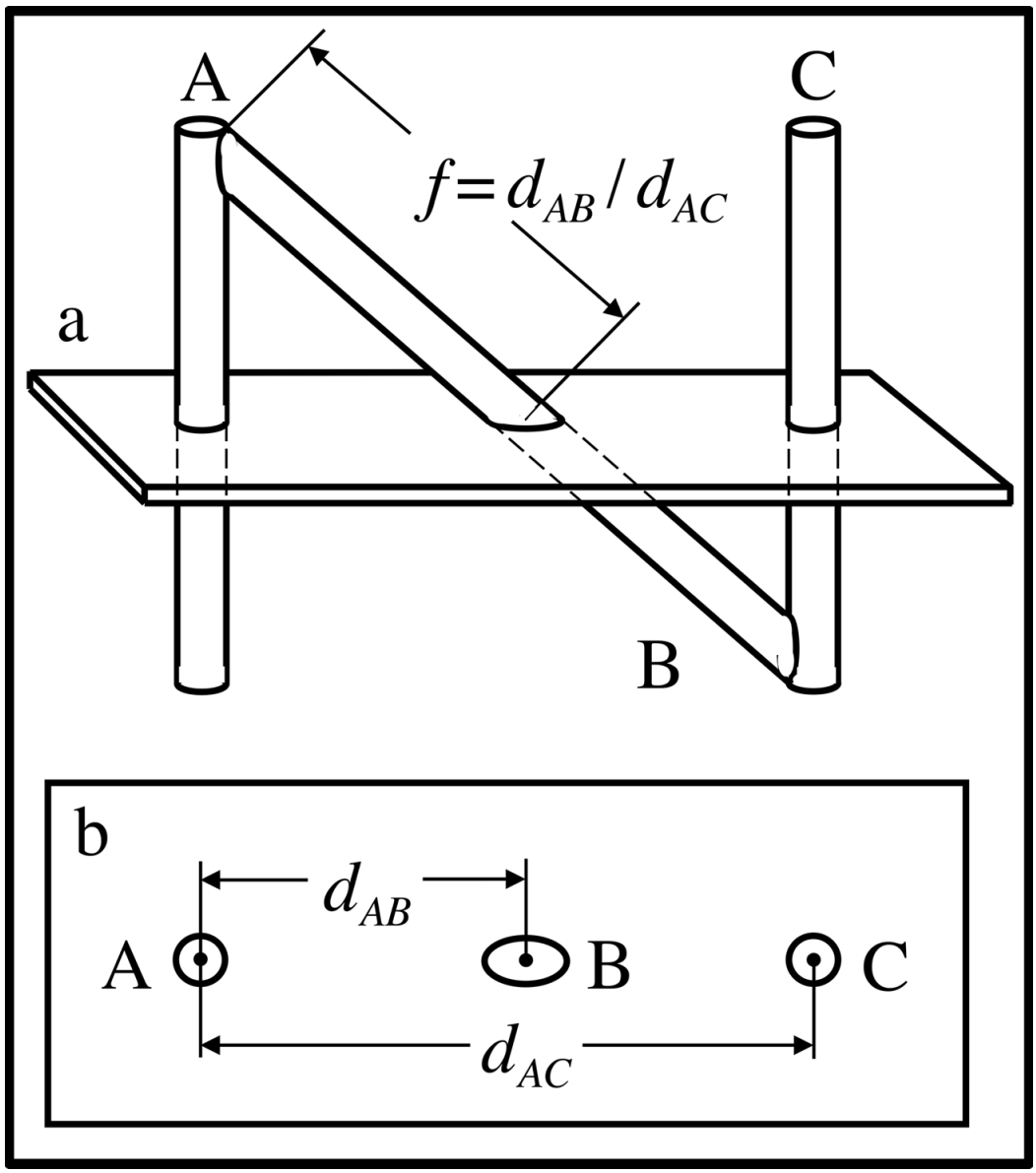

FIGURE 2: Intersection of the tomographic section with the N-localizer

$(\mathbf{a})$ Side view of the N-localizer. The tomographic section intersects rods A, B and C. $(\mathbf{b})$ Tomographic image. The intersection of the tomographic section with rods A, B and C creates fiducial circles A and C and fiducial ellipse B in the tomographic image. The distance d_{AB} between the centers of circle A and ellipse B and the distance d_{AC} between the centers of circles A and C are used to calculate the ratio $f = d_{AB}/d_{AC}$. This ratio represents the fraction of diagonal rod B that extends from the top of rod A to the point of intersection of rod B with the tomographic section. These geometric relationships are valid even if the vertical rods are not normal to the tomographic section, as can be demonstrated using similar triangles [1].

The fraction f is used to calculate the (x, y, z) coordinates of the point of intersection P'_B between rod B and the tomographic section (Figure 3). In this figure, points P'_A and P'_C represent the beginning and end, respectively, of the vector that extends from the top of rod A to the bottom of rod C. This vector coincides with the long axis of rod B. The (x_A, y_A, z_A) coordinates of the beginning point P'_A and the (x_C, y_C, z_C) coordinates of the end point

P'_C are known from the physical dimensions of the N-localizer. Hence, linear interpolation may be used to blend points P'_A and P'_C to obtain the (x_B, y_B, z_B) coordinates of the point of intersection P'_B between the long axis of rod B and the tomographic section

$$P'_B = P'_A + f\,(P'_C - P'_A) = f P'_C + (1 - f)\,P'_A \qquad (1)$$

The vector form of Equation 1 shows explicitly the (x, y, z) coordinates of points P'_A, P'_B and P'_C

$$\left[x_B\ y_B\ z_B\right] = f\left[x_C\ y_C\ z_C\right] + (1 - f)\left[x_A\ y_A\ z_A\right] \qquad (2)$$

Equation 1 or 2 may be used to calculate the (x_B, y_B, z_B) coordinates of the point of intersection P'_B between the long axis of rod B and the tomographic section. The point P'_B, which lies on the long axis of rod B in the three-dimensional coordinate system of the N-localizer, corresponds to the analogous point P_B, which lies at the center of ellipse B in the two-dimensional coordinate system of the tomographic image. Hence, there is a one-to-one correspondence between a point from the N-localizer and a point from the tomographic image.

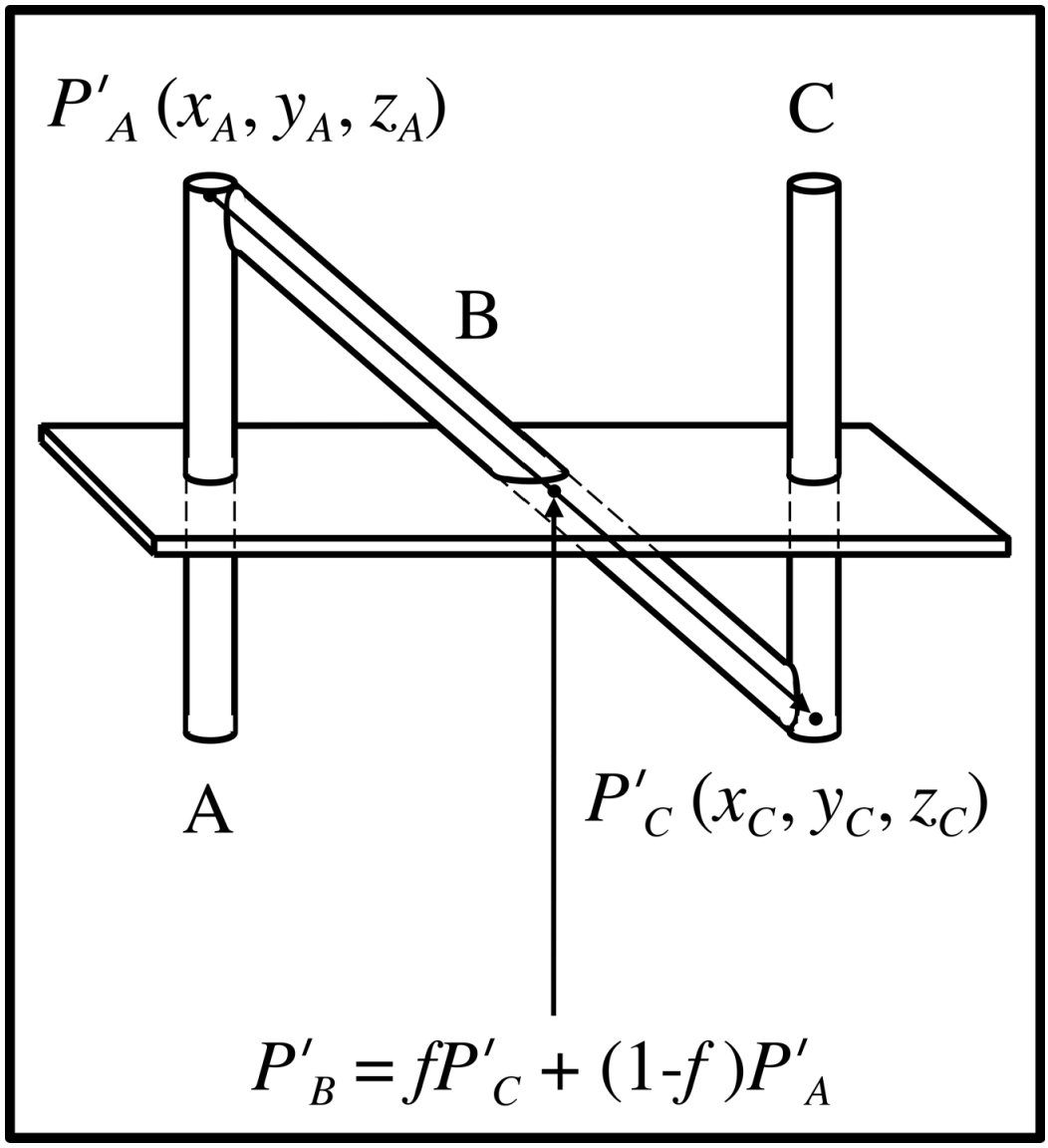

FIGURE 3: Calculation of the point of intersection between the

rod B and the tomographic section

The long axis of rod B is represented by a vector that extends from point P'_A at the top of rod A to point P'_C at the bottom of rod C. The (x_A, y_A, z_A) coordinates of point P'_A and the (x_C, y_C, z_C) coordinates of point P'_C are known from the physical dimensions of the N-localizer. Hence, the ratio $f = d_{AB}/d_{AC}$ may be used to blend the (x_A, y_A, z_A) and (x_C, y_C, z_C) coordinates of points P'_A and P'_C via linear interpolation as indicated by Equations 1 and 2. This interpolation calculates the (x_B, y_B, z_B) coordinates of the point of intersection P'_B between the long axis of rod B and the tomographic section.

The attachment of three N-localizers to a stereotactic frame (Figure *1*) permits calculation of the $(x_{B_1}, y_{B_1}, z_{B_1})$, $(x_{B_2}, y_{B_2}, z_{B_2})$ and $(x_{B_3}, y_{B_3}, z_{B_3})$ coordinates for the three respective points P'_{B_1}, P'_{B_2} and P'_{B_3} in the three-dimensional coordinate system of the stereotactic frame. These three points correspond respectively to the three analogous points P_{B_1}, P_{B_2}, and P_{B_3} in the two-dimensional coordinate system of the tomographic image. In the following discussion, the symbols P'_1, P'_2, and P'_3 will be used as a shorthand notation for P'_{B_1}, P'_{B_2}, and P'_{B_3}. The symbols P_1, P_2, and P_3 will be used as a shorthand notation for P_{B_1}, P_{B_2}, and P_{B_3}.

The three points P'_1, P'_2, and P'_3 lie on the long axes of the three respective diagonal rods B_1, B_2, and B_3 and have respective (x_1, y_1, z_1), (x_2, y_2, z_2), and (x_3, y_3, z_3) coordinates in the three-dimensional coordinate system of the stereotactic frame (Figure *4*). The analogous three points P_1, P_2, and P_3 lie at the centers of the three respective ellipses B_1, B_2, and B_3 and have (u_1, v_1), (u_2, v_2), and (u_3, v_3) coordinates in the two-dimensional coordinate system of the tomographic image (Figure *5*) and (Figure *6*). Because three points determine the orientation of a plane in three-dimensional space, the three coordinates (x_1, y_1, z_1), (x_2, y_2, z_2), and (x_3, y_3, z_3) together with the three coordinates (u_1, v_1), (u_2, v_2), and (u_3, v_3) determine the spatial orientation of the tomographic section relative to the stereotactic frame. This spatial orientation permits calculation of the (x_T, y_T, z_T) coordinates of a target point P'_T in the three-dimensional coordinate system of the stereotactic frame, given the (u_T, v_T) coordinates of the analogous target point P_T in the two-dimensional coordinate system of the tomographic image.

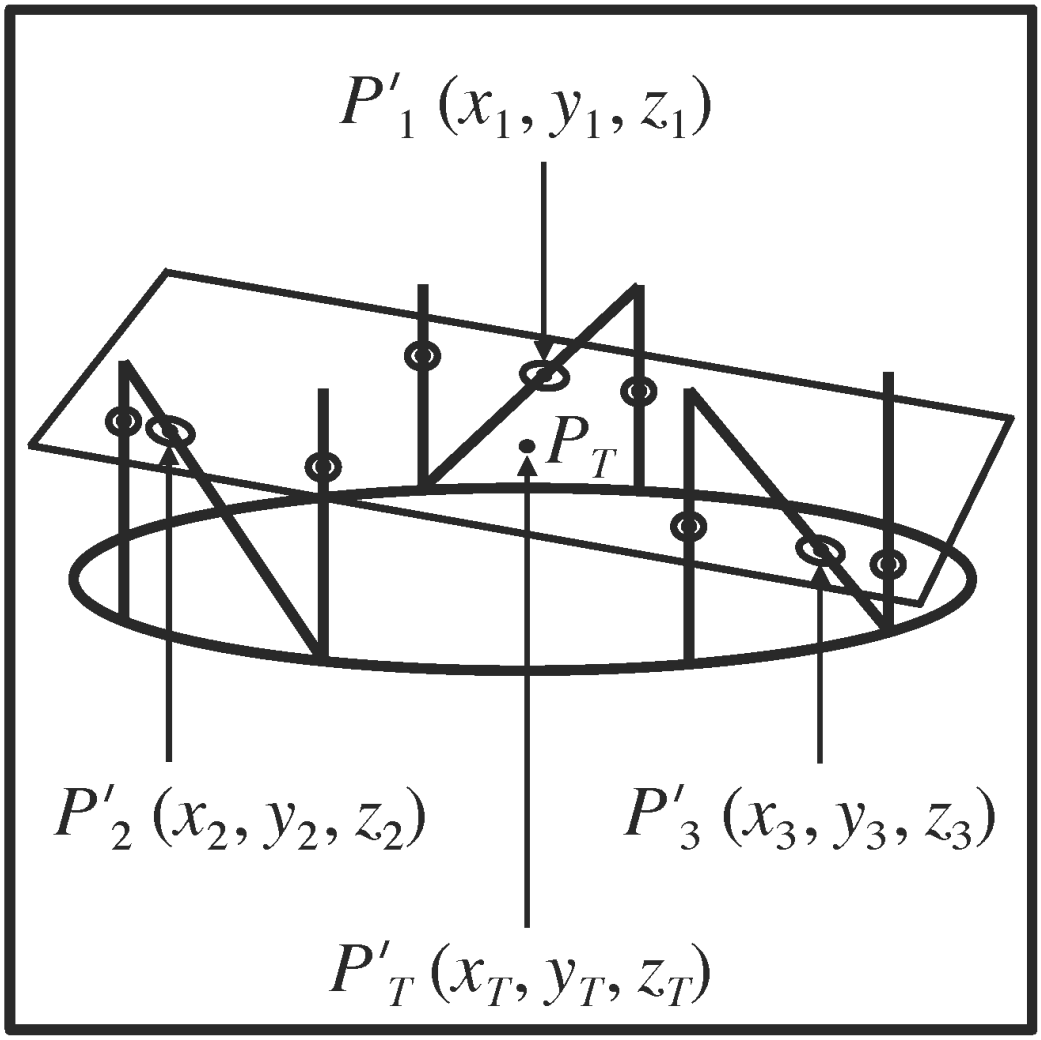

FIGURE 4: Representation of the tomographic section in the three-dimensional coordinate system of the stereotactic frame

The quadrilateral represents the tomographic section. The large oval depicts the base of the stereotactic frame. The vertical and diagonal lines that are attached to the large oval represent the nine rods. The centers of the six fiducial circles and the three fiducial ellipses that are created in the tomographic image by these nine rods are shown as points that lie in the tomographic section. The tomographic section intersects the long axes of the three diagonal rods at points P'_1, P'_2 and P'_3 that coincide with the respective centers P_1, P_2 and P_3 of the three ellipses (Figure 6). The (x_1, y_1, z_1), (x_2, y_2, z_2) and (x_3, y_3, z_3) coordinates of the respective points of intersection P'_1, P'_2 and P'_3 are calculated in the three-dimensional coordinate system of the stereotactic frame using Equations 1 and 2. Because these three points determine the spatial orientation of a plane in three-dimensional space, the spatial orientation of the tomographic section is determined relative to the stereotactic frame. The target point P'_T lies in the tomographic section. The (x_T, y_T, z_T) coordinates of this target point are calculated in the three-dimensional coordinate system of the stereotactic frame using Equation 5.

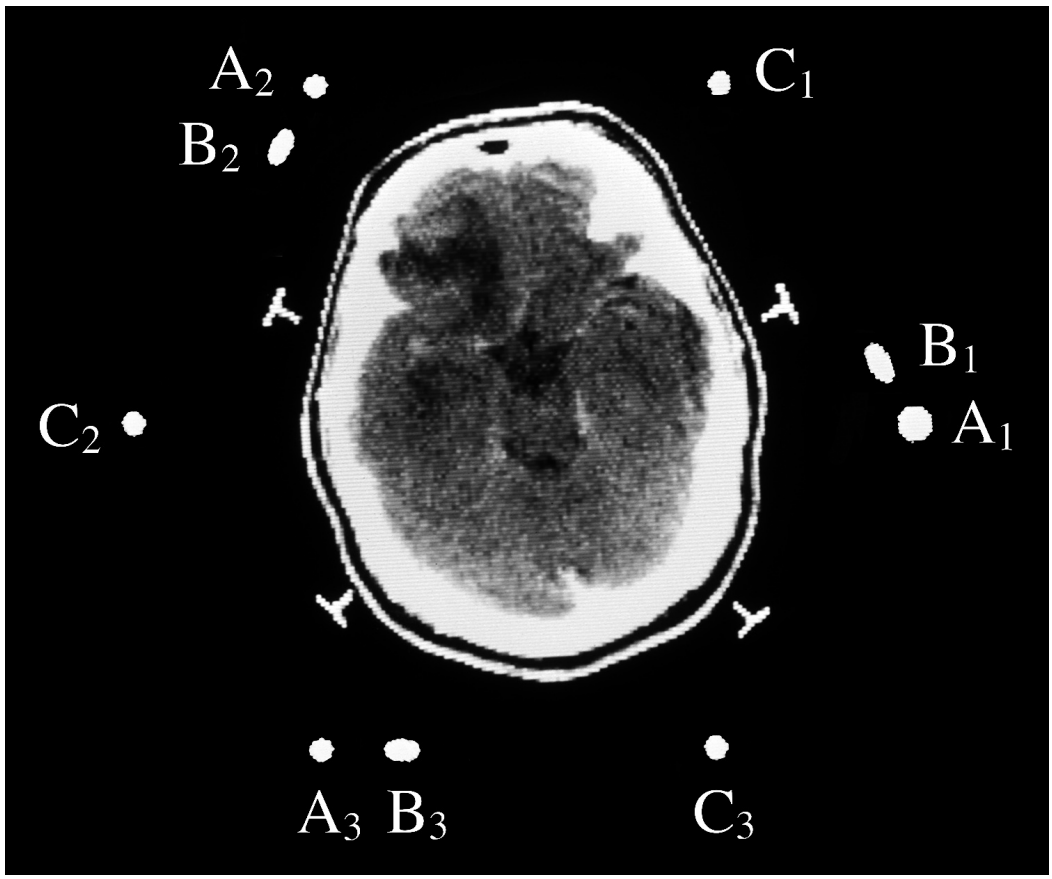

FIGURE 5: CT image with three sets of fiducials

CT image of a patient to whom a BRW CT localizer frame (Integra Radionics Inc., Burlington, MA) is attached. The cross sections of three N-localizers create three sets of fiducials $\{A_1, B_1, C_1\}$, $\{A_2, B_2, C_2\}$ and $\{A_3, B_3, C_3\}$ in the CT image. The large vertical rod A_1 allows it to be unambiguously distinguished from the other vertical rods and provides a visual cue that Figure 6 is rotated approximately 90 degrees counterclockwise relative to Figure 5 [7, 44]. The practice of including one large vertical rod in a CT localizer frame was extended to MR by placing an aluminum rod inside one of the hollow rods that are filled with petroleum jelly in an MR localizer frame [21].

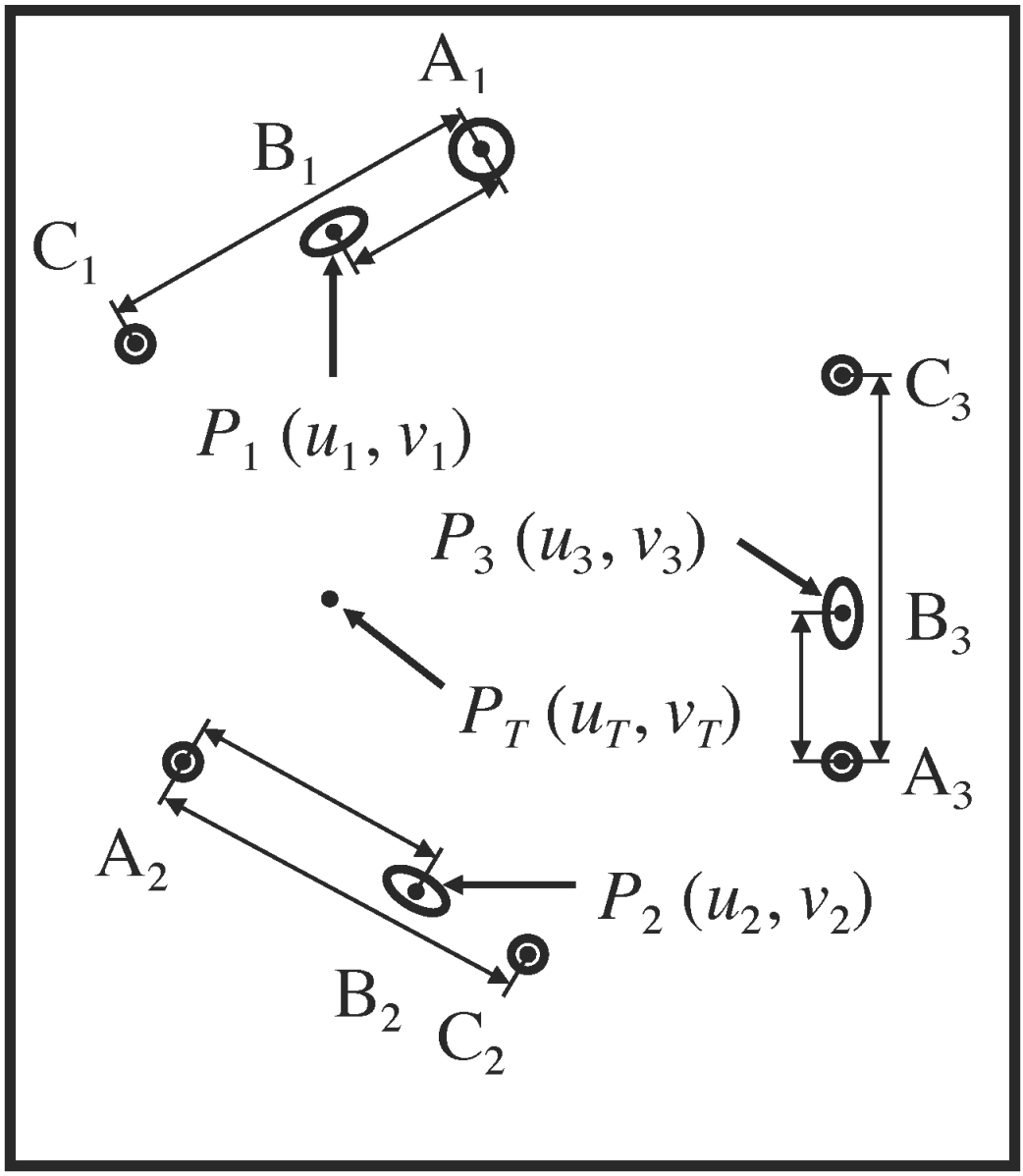

FIGURE 6: Representation of the two-dimensional coordinate system of the tomographic image

The cross sections of three N-localizers create three sets of fiducials $\{\mathrm{A}_1, \mathrm{B}_1, \mathrm{C}_1\}$, $\{\mathrm{A}_2, \mathrm{B}_2, \mathrm{C}_2\}$ and $\{\mathrm{A}_3, \mathrm{B}_3, \mathrm{C}_3\}$ in a tomographic image. Each set contains two circles and one ellipse that are collinear. For each set, the short double-ended arrows indicate the distance d_{AB} between the centers of circle A and ellipse B and the long double-ended arrows indicate the distance d_{AC} between the centers of circles A and C. The centers P_1, P_2 and P_3 of the three ellipses coincide with the respective points of intersection P_1', P_2' and P_3' of the long axes of the three diagonal rods with the tomographic section (Figure 4). The (u_1, v_1), (u_2, v_2) and (u_3, v_3) coordinates of the centers P_1, P_2 and P_3 correspond respectively to the (x_1, y_1, z_1), (x_2, y_2, z_2) and (x_3, y_3, z_3) coordinates of the points of intersection P_1', P_2' and P_3'. A target point P_T has (u_T, v_T) coordinates in the two-dimensional coordinate system of the scan image. The (x_T, y_T, z_T) coordinates of the analogous target point P_T' are calculated in the three-dimensional coordinate system of the stereotactic frame using Equation 5.

In order to facilitate calculation of the (x_T, y_T, z_T) coordinates of a target point P'_T, it is convenient to project the (u_1, v_1), (u_2, v_2), and (u_3, v_3) coordinates of the three respective points P_1, P_2, and P_3 onto the $w = 1$ plane in three-dimensional space by appending a third coordinate $w = 1$ to create $(u_1, v_1, 1)$, $(u_2, v_2, 1)$, and $(u_3, v_3, 1)$ coordinates. The w-coordinate may be set arbitrarily to any non-zero value, e.g., 1, so long as same value of w is used for each of the three w-coordinates [44]. The equations that are presented in the remainder of this article assume that a value of $w = 1$ has been used to project the (u_1, v_1), (u_2, v_2), and (u_3, v_3) coordinates. If a value of $w \neq 1$ were used instead of $w = 1$ to project the (u_1, v_1), (u_2, v_2), and (u_3, v_3) coordinates, the equations that are presented in the remainder of this article would no longer apply and would require revision so that the calculations that these equations describe may produce correct results.

The transformation from the two-dimensional coordinate system of the tomographic image into the three-dimensional coordinate system of the stereotactic frame may be represented using the three (x, y, z) and $(u, v, 1)$ coordinate pairs (x_1, y_1, z_1) and $(u_1, v_1, 1)$; (x_2, y_2, z_2) and $(u_2, v_2, 1)$; and (x_3, y_3, z_3) and $(u_3, v_3, 1)$ in the matrix equation

$$\begin{bmatrix} x_1 & y_1 & z_1 \\ x_2 & y_2 & z_2 \\ x_3 & y_3 & z_3 \end{bmatrix} = \begin{bmatrix} u_1 & v_1 & 1 \\ u_2 & v_2 & 1 \\ u_3 & v_3 & 1 \end{bmatrix} \begin{bmatrix} m_{11} & m_{12} & m_{13} \\ m_{21} & m_{22} & m_{23} \\ m_{31} & m_{32} & m_{33} \end{bmatrix} \qquad (3)$$

Equation 3 represents concisely a system of nine simultaneous linear equations that determine the spatial orientation of the tomographic section relative to the stereotactic frame. This equation transforms the $(u_1, v_1, 1)$, $(u_2, v_2, 1)$, and $(u_3, v_3, 1)$ coordinates from the two-dimensional coordinate system of the tomographic image to create (x_1, y_1, z_1), (x_2, y_2, z_2), and (x_3, y_3, z_3) coordinates in the three-dimensional coordinate system of the stereotactic frame.

An analogy provides insight into how the transformation of Equation 3 operates. Consider the tomographic image to be an elastic membrane. The transformation describes the processes of stretching the membrane in the plane of the tomographic image, rotating the membrane about an axis that is normal to the plane of the tomographic image, flipping the membrane side-to-side if necessary, tilting the membrane if necessary so that it is not parallel to the base of the stereotactic frame, and lastly, lifting the membrane into place upon the scaffold of the three N-localizers such that the three points P_1, P_2, and P_3 from the tomographic image precisely coincide with the respective three points P'_1, P'_2, and P'_3 from the stereotactic frame. Then *any* other point that lies on the membrane, for example, the target point P_T, is transformed by the same stretching, rotating, flipping, tilting, and lifting processes that transformed the three points P_1, P_2, and P_3. In this manner, the (u_T, v_T) coordinates of the target point P_T may be transformed from the two-dimensional coordinate system of the tomographic image into the three-dimensional coordinate system of the stereotactic frame to produce the (x_T, y_T, z_T) coordinates of the analogous target point P'_T. The ability to transform coordinates in this manner obviates the need to rigidly fix the stereotactic frame to the tomographic scanner in order to guarantee that the tomographic section is parallel to the base of the stereotactic frame.

In Equation 3, the matrix elements x_1, y_1, z_1, x_2, y_2, z_2, x_3, y_3, and z_3 as well as the matrix elements u_1, v_1, u_2, v_2, u_3, and v_3 are known. The matrix elements m_{11} through m_{33} are unknown; hence, Equation 3 may be inverted to solve for these unknown elements of the transformation matrix

$$\begin{bmatrix} m_{11} & m_{12} & m_{13} \\ m_{21} & m_{22} & m_{23} \\ m_{31} & m_{32} & m_{33} \end{bmatrix} = \begin{bmatrix} u_1 & v_1 & 1 \\ u_2 & v_2 & 1 \\ u_3 & v_3 & 1 \end{bmatrix}^{-1} \begin{bmatrix} x_1 & y_1 & z_1 \\ x_2 & y_2 & z_2 \\ x_3 & y_3 & z_3 \end{bmatrix} \qquad (4)$$

where the exponent "-1" indicates the inverse of the matrix that contains the elements u_1, v_1, u_2, v_2, u_3, and v_3.

Once the transformation matrix elements m_{11} through m_{33} are known, the (u_T, v_T) coordinates of the target point P_T may be transformed from the two-dimensional coordinate system of the tomographic image into the three-dimensional coordinate system of the stereotactic frame to obtain the (x_T, y_T, z_T) coordinates of the analogous target point P'_T

$$\begin{bmatrix} x_T & y_T & z_T \end{bmatrix} = \begin{bmatrix} u_T & v_T & 1 \end{bmatrix} \begin{bmatrix} m_{11} & m_{12} & m_{13} \\ m_{21} & m_{22} & m_{23} \\ m_{31} & m_{32} & m_{33} \end{bmatrix} \qquad (5)$$

The above review of the mathematics of the N-localizer is sufficient to permit the presentation of new developments below.

Materials And Methods

Some applications of the N-localizer have used four N-localizers to produce four sets of fiducials in a CT image [5, 9, 16, 19, 32, 40]. Four sets of fiducials are visible in the CT image of Figure 7. The transformation from the two-dimensional coordinate system of this tomographic image into the three-dimensional coordinate system of the stereotactic frame may be represented as

$$\begin{bmatrix} x_1 & y_1 & z_1 \\ x_2 & y_2 & z_2 \\ x_3 & y_3 & z_3 \\ x_4 & y_4 & z_4 \end{bmatrix} = \begin{bmatrix} u_1 & v_1 & 1 \\ u_2 & v_2 & 1 \\ u_3 & v_3 & 1 \\ u_4 & v_4 & 1 \end{bmatrix} \begin{bmatrix} m_{11} & m_{12} & m_{13} \\ m_{21} & m_{22} & m_{23} \\ m_{31} & m_{32} & m_{33} \end{bmatrix} \qquad (6)$$

An important distinction between Equations 3 and 6 is that Equation 3 may be inverted via Equation 4 to solve for the transformation matrix elements m_{11} through m_{33}, whereas Equation 6 may not be inverted to obtain these transformation matrix elements because Equation 6 includes non-square matrices [44].

One solution to this problem is to ignore one of the four sets of fiducials and to use the remaining three sets of fiducials for Equation 4. This solution raises a question concerning which set of fiducials to ignore. One approach to ignoring a set of fiducials is to attempt to minimize errors by choosing the three fiducial points $\mathrm{B_i}$ that form a triangle that encloses the target point P_T [5]. For example, in Figure 5 the target point lies within the triangle $\mathrm{B_1B_2B_3}$ so fiducial $\mathrm{B_4}$ would be ignored for application of Equation 4. Although this approach aims to minimize errors, it requires that important data, i.e., one set of fiducials, be ignored.

It is possible to minimize error via the method of least squares [46] without ignoring any of the fiducials. The least-squares approach applies to three or more sets of fiducials. The equations that are required for least-squares minimization are obtained by first expanding the matrix

multiplication of Equation 6 and expressing the result for the matrix elements x_i , y_i and z_i

$$\begin{aligned} x_i &= u_i m_{11} + v_i m_{21} + m_{31} \\ y_i &= u_i m_{12} + v_i m_{22} + m_{32} \\ z_i &= u_i m_{13} + v_i m_{23} + m_{33} \end{aligned} \qquad (7)$$

where the subscript i designates the matrix row. In the presence of error, Equation 7 may be modified to express the errors in x_i , y_i and z_i , respectively, as δx_i , δy_i and δz_i

$$\begin{aligned} \delta x_i &= x_i - u_i m_{11} - v_i m_{21} - m_{31} \\ \delta y_i &= y_i - u_i m_{12} - v_i m_{22} - m_{32} \\ \delta z_i &= z_i - u_i m_{13} - v_i m_{23} - m_{33} \end{aligned} \qquad (8)$$

In order to minimize these errors via the method of least squares, the values of δx_i , δy_i and δz_i are squared to obtain the error functions E_x , E_y and E_z

$$\begin{aligned} E_x\left(m_{11}, m_{21}, m_{31}\right) &= \sum \left(x_i - u_i m_{11} - v_i m_{21} - m_{31}\right)^2 \\ E_y\left(m_{12}, m_{22}, m_{32}\right) &= \sum \left(y_i - u_i m_{12} - v_i m_{22} - m_{32}\right)^2 \\ E_z\left(m_{13}, m_{23}, m_{33}\right) &= \sum \left(z_i - u_i m_{13} - v_i m_{23} - m_{33}\right)^2 \end{aligned} \qquad (9)$$

The following discussion illustrates minimization of the error function E_x ; minimization of the error functions E_y and E_z is performed in an analogous manner. At the minimum of a function, all of the derivatives are equal to zero. Evaluating the derivatives $\partial E_x/\partial m_{11}$, $\partial E_x/\partial m_{21}$ and $\partial E_x/\partial m_{31}$ and setting the resulting expressions for these derivatives to zero yields

$$\begin{aligned} \partial E_x/\partial m_{11} &= \sum 2\left(x_i - u_i m_{11} - v_i m_{21} - m_{31}\right) u_i = 0 \\ \partial E_x/\partial m_{21} &= \sum 2\left(x_i - u_i m_{11} - v_i m_{21} - m_{31}\right) v_i = 0 \\ \partial E_x/\partial m_{31} &= \sum 2\left(x_i - u_i m_{11} - v_i m_{21} - m_{31}\right) = 0 \end{aligned} \qquad (10)$$

Simplifying and rearranging the above equations for the derivatives yields a system of three simultaneous linear equations of the three unknowns m_{11} , m_{21} and m_{31}

$$\begin{aligned} m_{11} \sum {u_i}^2 + m_{21} \sum u_i v_i + m_{31} \sum u_i &= \sum u_i x_i \\ m_{11} \sum u_i v_i + m_{21} \sum {v_i}^2 + m_{31} \sum v_i &= \sum v_i x_i \\ m_{11} \sum u_i + m_{21} \sum v_i + m_{31} n &= \sum x_i \end{aligned} \qquad (11)$$

where n is the number of sets of fiducials; in the case of Equation 6, $n = 4$. These simultaneous linear equations may be solved using Cramer's rule [47] to yield the matrix elements m_{11} , m_{21} and m_{31} that minimize the error function E_x as follows. Each of the elements m_{11} , m_{21} and m_{31} that are found in the first column of the transformation matrix and that minimize E_x may be calculated as the ratio of two determinants wherein the denominator determinant contains the sums from Equation 11

$$\begin{vmatrix} \sum {u_i}^2 & \sum u_i v_i & \sum u_i \\ \sum u_i v_i & \sum {v_i}^2 & \sum v_i \\ \sum u_i & \sum v_i & n \end{vmatrix} \qquad (12)$$

and wherein the numerator determinant for the calculation of m_{11} , m_{21} and m_{31} , respectively, is obtained by replacing the first, second and third columns of Equation 12 with

$$\begin{bmatrix} \sum u_i x_i \\ \sum v_i x_i \\ \sum x_i \end{bmatrix} \qquad (13)$$

Similarly, each of the elements m_{12} , m_{22} and m_{32} that are found in the second column of the transformation matrix and that minimize E_y may be calculated as the ratio of two determinants wherein the denominator determinant is shown in Equation 12 and wherein the numerator determinant for the calculation of m_{12} , m_{22} and m_{32} , respectively, is obtained by replacing the first, second and third columns of Equation 12 with

$$\begin{bmatrix} \sum u_i y_i \\ \sum v_i y_i \\ \sum y_i \end{bmatrix} \qquad (14)$$

Finally, each of the elements m_{13} , m_{23} and m_{33} that are found in the third column of the transformation matrix and that minimize E_z may be calculated as the ratio of two determinants wherein the denominator determinant is shown in Equation 12 and wherein the numerator determinant for the calculation of m_{13} , m_{23} and m_{33} , respectively, is obtained by replacing the first, second and third columns of Equation 12 with

$$\begin{bmatrix} \sum u_i z_i \\ \sum v_i z_i \\ \sum z_i \end{bmatrix} \qquad (15)$$

In this manner, the nine elements of the transformation matrix may be obtained such that these matrix elements minimize the error functions E_x , E_y and E_z .

Once the elements of the transformation matrix have been calculated as discussed above, the transformation matrix may be used as shown in Equation 5 to transform the (u_T, v_T) coordinates of the target point P_T from the two-dimensional coordinate system of the tomographic image into the three-dimensional coordinate system of the stereotactic frame to obtain the (x_T, y_T, z_T) coordinates of the analogous target point P'_T .

The accuracy of the calculation of the transformation matrix elements, and hence the accuracy of the transformation of the (u_T, v_T) coordinates, is indicated by the correlation coefficient r_{xyz} that is a measure of how well the (x_i, y_i, z_i) coordinates fit a plane equation

This correlation coefficient may be obtained by first calculating the three linear correlation coefficients r_{xz} , r_{yz} and r_{xy} in the manner that is shown below for r_{xy} [48]

$$r_{xy} = \frac{n\sum x_i y_i - \sum x_i \sum y_i}{\sqrt{n\sum {x_i}^2 - \left(\sum x_i\right)^2}\sqrt{n\sum {y_i}^2 - \left(\sum y_i\right)^2}} \qquad (17)$$

then combining these linear correlation coefficients to obtain a coefficient of multiple correlation [49]

$$r_{xyz} = \sqrt{\frac{{r_{xz}}^2 + {r_{yz}}^2 - 2r_{xz}r_{yz}r_{xy}}{1 - {r_{xy}}^2}} \qquad (18)$$

Results

Figure 7 is a CT image wherein four N-localizers have produced four sets of fiducials. A cursor was centered over the cross hairs for each of the eight fiducials and for the target point P_T in order to read the (u, v) coordinates of the fiducials and the target point. These coordinates are shown in Table 1.

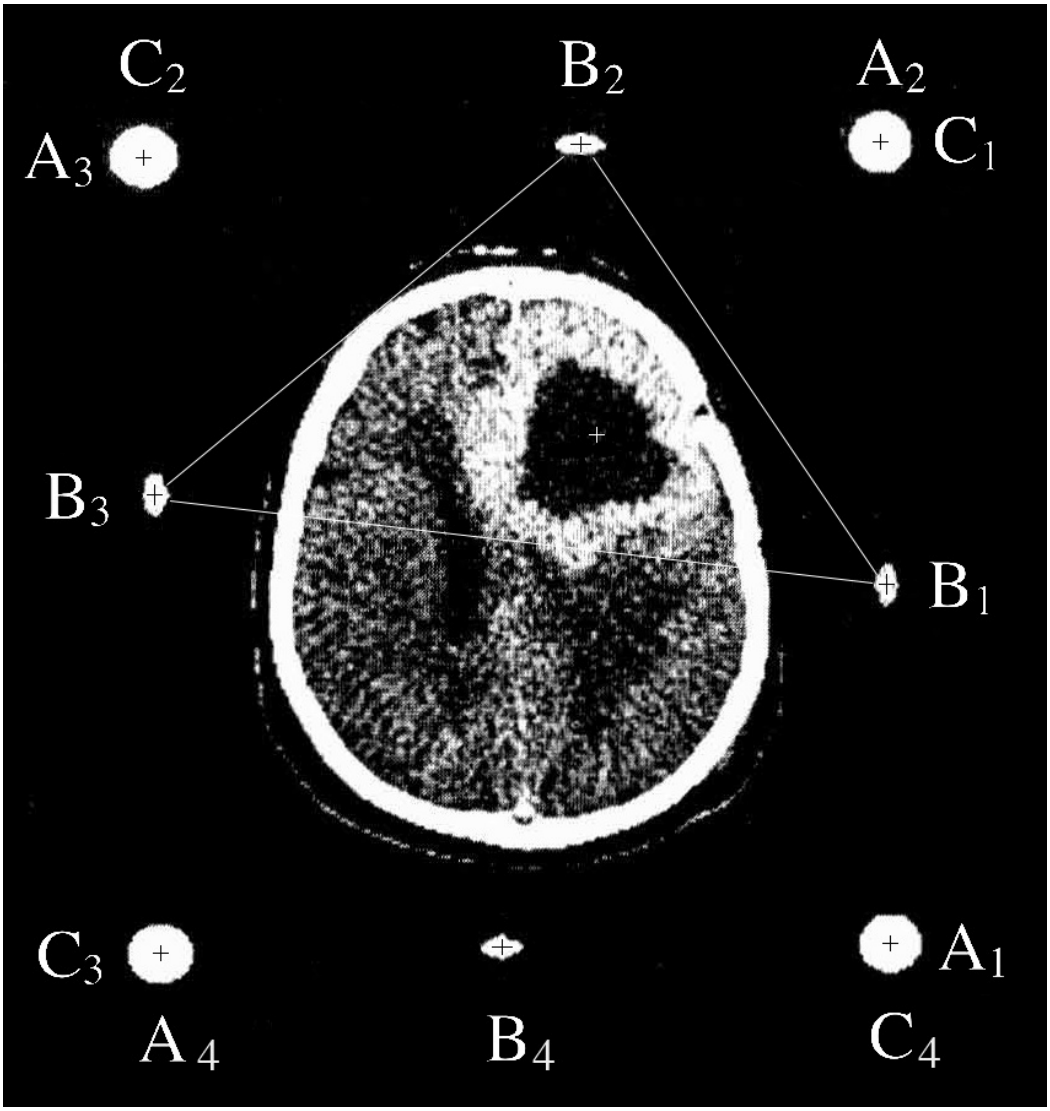

FIGURE 7: CT image with four sets of fiducials

Four N-localizers create four sets of fiducials $\{A_1, B_1, C_1\}$, $\{A_2, B_2, C_2\}$, $\{A_3, B_3, C_3\}$ and $\{A_4, B_4, C_4\}$ in the CT image. The N-localizers are merged end-to-end such that $A_2 = C_1$, $A_3 = C_2$, $A_4 = C_3$ and $A_1 = C_4$. The black cross hairs indicate the centers of the fiducials and the white cross hairs indicate the target point P_T that lies inside the triangle $B_1B_2B_3$ (see text for explanation). Adapted from [5].

Cross Hair	u	v
$\mathrm{A}_1 = \mathrm{C}_4$	2.409	2.553
B_1	2.397	1.577
$\mathrm{A}_2 = \mathrm{C}_1$	2.382	0.374
B_2	1.567	0.382
$\mathrm{A}_3 = \mathrm{C}_2$	0.380	0.418
B_3	0.411	1.336
$\mathrm{A}_4 = \mathrm{C}_3$	0.429	2.581
B_4	1.354	2.566
P_T	1.612	1.171

TABLE 1: (u, v) coordinates of fiducials and target point P_T from Figure 7

The (u, v) coordinates of the fiducials and the target point P_T were measured by centering a cursor over the cross hairs in the CT image of Figure 7. The position of the reference origin of the CT image and the units of measurement of u_i and v_i (millimeters, pixels, etc.) are irrelevant, so long as the same reference origin and units of measurement are used to measure each u_i and v_i. Also, independent of whether the u-coordinates are measured in the horizontal direction and the v-coordinates are measured in the vertical direction, or $vice\ versa$, Equation 5 will calculate the same (x_T, y_T, z_T) coordinates for the analogous target point P'_T [44].

In order to calculate a transformation matrix from the data in Table 1, the (x, y, z) coordinates of the points at each end of the four diagonal rods B_1, B_2, B_3, and B_4 must be known in the three-dimensional coordinate system of the stereotactic frame so that the points of intersection between the long axes of these rods and the tomographic section may be calculated using Equation 1 or 2. The author does not have access to the stereotactic frame that is visible in the CT image of Figure 7, so the (x, y, z) coordinates of these eight points are not known. However, for the purposes of this article, a sufficient model of this stereotactic frame is a cube whose edges are 30 cm long and wherein the vertical rods A_1, A_2, A_3, and A_4 form the vertical edges of the cube. Then the beginning point of diagonal rod B_1 is assigned from the point at the top of vertical rod A_1 and the end point of diagonal rod B_1 is assigned from the point at the bottom of vertical rod A_2. The beginning and end points of diagonal rods B_2, B_3, and B_4 are assigned in a similar manner.

Based on the above assumptions regarding the physical dimensions of the stereotactic frame and using the (u_i, v_i) coordinates from Table 1, a transformation matrix was calculated using all four fiducials B_1, B_2, B_3, and B_4 by solving Equation 6 via Equations 12-15. Then this transformation matrix was used to transform the (u_T, v_T) coordinates of the target point P_T that are shown in Table 1 into the (x_T, y_T, z_T) coordinates for the analogous target point $P'_{T(4)}$ that are shown in Table 2. The correlation coefficient $r_{xyz} = 0.99998$ was calculated to indicate the accuracy of the transformation.

In order to assess the effect of ignoring one set of fiducials upon the accuracy of the transformation, a different transformation matrix was calculated via Equation 4 using the

(u_i, v_i) coordinates from Table 1 for each of the four combinations of fiducials $B_1B_2B_3$, $B_2B_3B_4$, $B_3B_4B_1$, and $B_4B_1B_2$. Then these four different transformation matrices were used to transform the (u_T, v_T) coordinates of the target point P_T that are shown in Table 1 into (x_T, y_T, z_T) coordinates for the four different target points $P'_{T(3)}$ that are shown in Table 2. Also, the Pythagorean distance d, i.e., the transformation error, between each of these four target points $P'_{T(3)}$ and the target point $P'_{T(4)}$ was calculated. The mean transformation error is 0.587 mm and the standard deviation is 0.313 mm.

Target Point and Fiducials	x (cm)	y (cm)	(cm)	d (mm)
$P'_{T(4)}$ $B_1B_2B_3B_4$	3.246	4.178	2.106	
$P'_{T(3)}$ $B_1B_2B_3$	3.235	4.199	2.105	0.237
$P'_{T(3)}$ $B_2B_3B_4$	3.278	4.120	2.107	0.663
$P'_{T(3)}$ $B_3B_4B_1$	3.206	4.252	2.103	0.847
$P'_{T(3)}$ $B_4B_1B_2$	3.265	4.143	2.107	0.399

TABLE 2: (x, y, z) coordinates of the target point P'_T calculated from Figure 7

The (x, y, z) coordinates in centimeters for the target point $P'_{T(4)}$ were calculated using all four fiducials B_1, B_2, B_3 and B_4 from Figure 7. Also, the (x, y, z) coordinates in centimeters for the four different target points $P'_{T(3)}$ were calculated using all four combinations of three fiducials. The Pythagorean distance d from $P'_{T(4)}$ to each $P'_{T(3)}$ is indicated in millimeters.

Figure 8 is a MR image wherein four N-localizers have produced four sets of fiducials. A cursor was centered over the cross hairs for each of the 12 fiducials and for the target point P_T in order to read the (u, v) coordinates of the fiducials and the target point. These coordinates are shown in Table 3.

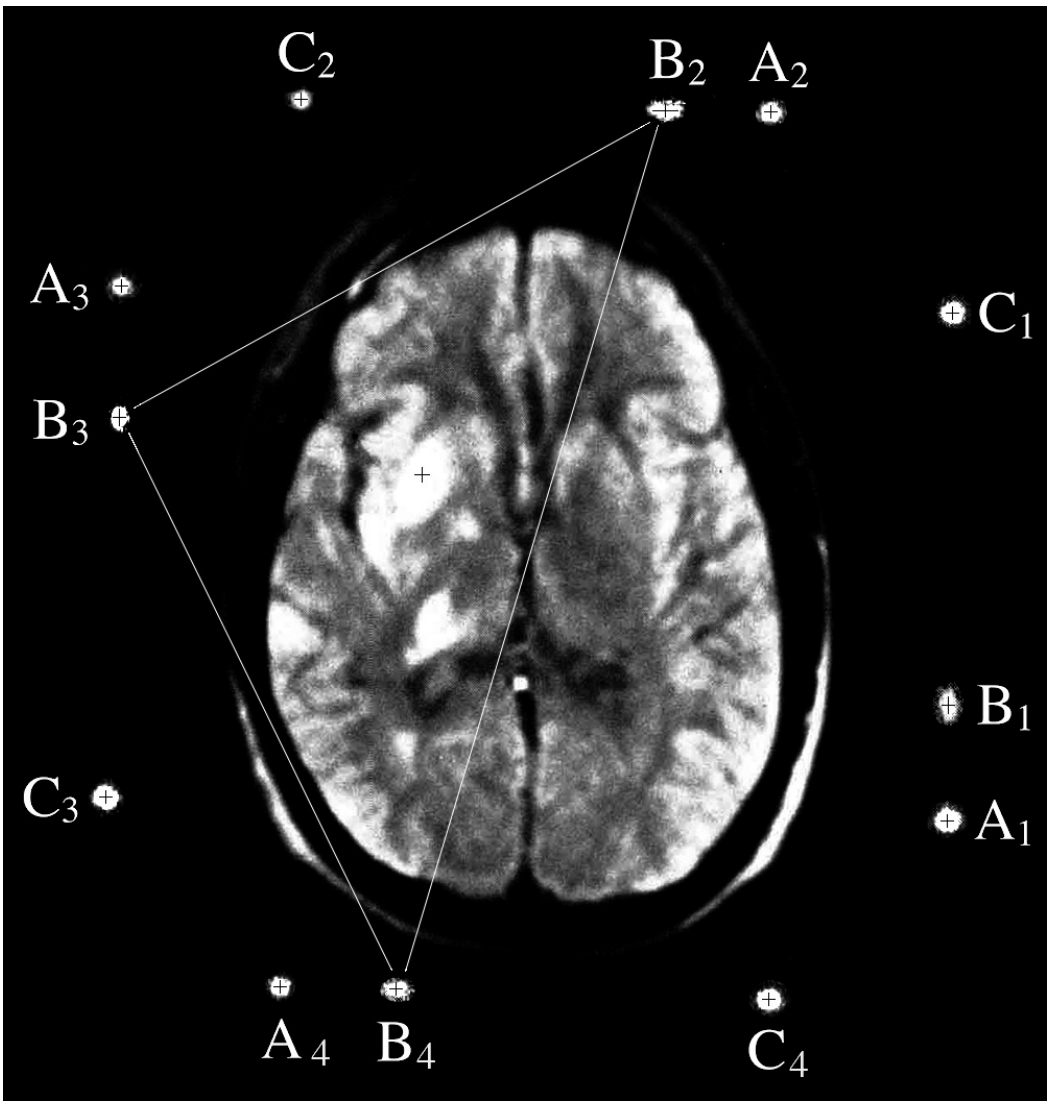

FIGURE 8: MR image with four sets of fiducials

MR image of a patient to whom a first-generation BRW MR localizer frame (Radionics Inc., Burlington, MA) is attached. Four N-localizers create four sets of fiducials $\{A_1, B_1, C_1\}$, $\{A_2, B_2, C_2\}$, $\{A_3, B_3, C_3\}$ and $\{A_4, B_4, C_4\}$ in the MR image. The black cross hairs indicate the centers of the fiducials and the target point P_T that lies inside the triangle $B_2B_3B_4$ (see text for explanation). Adapted from [19].

Cross Hair	u	v
A_1	3.014	2.604
B_1	3.018	2.234
C_1	3.030	0.981
A_2	2.451	0.338
B_2	2.114	0.334
C_2	0.950	0.298
A_3	0.378	0.894
B_3	0.371	1.314
C_3	0.328	2.528
A_4	0.884	3.134
B_4	1.254	3.141
C_4	2.444	3.174
P_T	1.337	1.499

TABLE 3: (u, v) coordinates of fiducials and target point P_T from Figure 8

The (u, v) coordinates of the fiducials and the target point P_T were measured by centering a cursor over the cross hairs in the CT image of Figure 8.

In a similar manner to the treatment of the data from Table 1, the (u_i, v_i) coordinates from Table 3 were used to calculate a transformation matrix using all four fiducials B_1, B_2, B_3, and B_4 by solving Equation 6 via Equations 12-15. Then this transformation matrix was used to transform the (u_T, v_T) coordinates of the target point P_T that are shown in Table 3 into the (x_T, y_T, z_T) coordinates for the analogous target point $P'_{T(4)}$ that are shown in Table 4. The correlation coefficient $r_{xyz} = 0.88976$ was calculated to indicate the accuracy of the transformation.

In order to assess the effect of ignoring one set of fiducials upon the accuracy of the transformation, a different transformation matrix was calculated via Equation 4 using the (u_i, v_i) coordinates from Table 3 for each of the four combinations of fiducials $B_1B_2B_3$, $B_2B_3B_4$, $B_3B_4B_1$, and $B_4B_1B_2$. Then these four different transformation matrices were used to transform the (u_T, v_T) coordinates of the target point P_T that are shown in Table 3 into (x_T, y_T, z_T) coordinates for the four different target points $P'_{T(3)}$ that are shown in Table 4. Also, the Pythagorean distance d, i.e., the transformation error, between each of these four target points $P'_{T(3)}$ and the target point $P'_{T(4)}$ was calculated. The mean transformation error is 2.149 mm and the standard deviation is 1.230 mm.

Target Point and Fiducials	x (cm)	y (cm)	(cm)	d (mm)
$P'_{T(4)}$ $B_1B_2B_3B_4$	-3.804	2.875	7.791	
$P'_{T(3)}$ $B_1B_2B_3$	-3.901	2.904	7.647	1.757
$P'_{T(3)}$ $B_2B_3B_4$	-3.755	2.860	7.863	0.886
$P'_{T(3)}$ $B_3B_4B_1$	-3.947	2.918	7.578	2.594
$P'_{T(3)}$ $B_4B_1B_2$	-3.619	2.819	8.065	3.358

TABLE 4: (x, y, z) coordinates of the target point P'_T calculated from Figure 8

The (x, y, z) coordinates in centimeters for the target point $P'_{T(4)}$ were calculated using all four fiducials B_1, B_2, B_3 and B_4 from Figure 8. Also, the (x, y, z) coordinates in centimeters for the four different target points $P'_{T(3)}$ were calculated using all four combinations of three fiducials. The Pythagorean distance d from $P'_{T(4)}$ to each $P'_{T(3)}$ is indicated in millimeters.

Discussion

For the CT image of Figure 7, the correlation coefficient $r_{xyz} = 0.99998$ and the mean transformation error of 0.587 mm indicate that only a small amount of error is present in the CT image. A possible source of this error is the fact that the (u, v) coordinates of the centers of the fiducials were recorded manually using a cursor and hence these coordinates are accurate to only the nearest pixel. In practice, this source of error is greatly reduced by computer software that calculates the center of each fiducial at sub-pixel precision instead of relying on a human to identify the center of the fiducial manually.

The attempt to minimize the transformation error by ignoring one set of fiducials [5] does diminish the error, as can be seen from Figure 7 and Table 2. Assuming that $P'_{T(4)}$, which was calculated using all four sets of fiducials, is the most accurate target point, it is evident that the Pythagorean distance d from $P'_{T(4)}$ to $P'_{T(3)}$ increases as the position of P_T relative to the triangle that is formed by the three B_i that are used for application of Equation 4 progresses from well inside triangle $B_1B_2B_3$ to marginally inside triangle $B_4B_1B_2$ to marginally outside triangle $B_2B_3B_4$ to well outside triangle $B_3B_4B_1$. Figure 8 and Table 4 show a similar trend of increasing Pythagorean distance d from $P'_{T(4)}$ to $P'_{T(3)}$ as the position of P_T progresses from well inside triangle $B_2B_3B_4$ to marginally inside triangle $B_1B_2B_3$ to marginally outside triangle $B_3B_4B_1$ to well outside triangle $B_4B_1B_2$. Because the Pythagorean distance d represents the transformation error, these trends demonstrate that the transformation error may be minimized to some extent by choosing the three fiducials B_i that form a triangle that encloses the target point P_T. However, choosing three of the four fiducials B_i ignores one set of fiducials and hence requires that important data be discarded, whereas least-squares minimization uses all four fiducials and thus discards no data.

For the MR image of Figure 8, the correlation coefficient $r_{xyz} = 0.88976$ and the mean transformation error of 2.149 mm indicate that substantially more error is present in the MR image of Figure 8 than in the CT image of Figure 7. A likely source of this error is nonlinear distortion of the MR image that may be caused by metallic elements of the stereotactic frame, inhomogeneity and temporal fluctuation of the magnetic field, and metallic equipment near

the MR scanner [18,19,21,28,33].

In view of the N-localizer's requirement for linearity, the susceptibility of MR to nonlinear distortion can potentially degrade the accuracy of MR-guided stereotactic surgery [44]. In the absence of nonlinear distortion, the centers of the two circles A_i and C_i and the ellipse B_i are expected to be collinear, as shown in Figure *6* [44]. Hence, it has been suggested that the linearity of an MR image may be checked by calculating a correlation coefficient $r_{uv(i)}$ for each of the four sets of fiducials $\{A_i, B_i, C_i\}$ using the (u, v) coordinates of the centers of the three fiducials A_i, B_i, and C_i as shown in Equation 17 [21]. However, this test for linearity is sensitive to nonlinear distortion only if the distortion causes the center of fiducial B_i to move perpendicularly to the line that connects the centers of fiducials A_i and C_i. This test for linearity is insensitive to the case where the distortion causes the center of fiducial B_i to move along the line that connects the centers of fiducials A_i and C_i because in this case the value of the correlation coefficient $r_{uv(i)}$ does not change.

On the other hand, the correlation coefficient r_{xyz} is sensitive to any displacement of the centers of fiducials B_i relative to the centers of fiducials A_i and C_i. Moreover, the correlation coefficient r_{xyz} is sensitive to the displacement of the center of any fiducial relative to the center of any other fiducial. Such a displacement alters the calculation of the (x_i, y_i, z_i) coordinates of one or more of the four P_i' via Equations 1 and 2, and those altered coordinates affect the correlation coefficient r_{xyz}.

Table *5* shows that the four correlation coefficients $r_{uv(i)}$ are insensitive to the nonlinear distortion that is present in the MR image of Figure *8*. The correlation coefficients $r_{uv(i)}$ that are calculated for each of the four sets of fiducials $\{A_i, B_i, C_i\}$ are substantially larger than the correlation coefficient r_{xyz} that is calculated using the four fiducials B_1, B_2, B_3 and B_4. This disparity between r_{xyz} and the four $r_{uv(i)}$ suggests that the distortion in the MR image of Figure *8* either causes the centers of the four fiducials B_i to move along the lines that connect the centers of fiducials A_i and C_i, or causes the four sets of fiducials $\{A_i, B_i, C_i\}$ to move relative to one another in a manner that does not affect the collinear relationship within each set of fiducials $\{A_i, B_i, C_i\}$.

Correlation Coefficient	Value
$r_{uv(1)}$	0.99973
$r_{uv(2)}$	0.99223
$r_{uv(3)}$	0.99276
$r_{uv(4)}$	0.99793
r_{xyz}	0.88976

TABLE 5: Correlation coefficients calculated from the fiducials of Figure 8

The correlation coefficients that are calculated from the (u, v) coordinates of the fiducials in the MR image of Figure 8 indicate that the correlation coefficients $r_{uv(i)}$ are insensitive to nonlinear distortion of this MR image, whereas the correlation coefficient r_{xyz} is sensitive to that distortion.

Four or more N-localizers require the use of Equations 12-15 instead of Equation 4 to calculate

the transformation matrix. For three N-localizers, either Equation 4 or Equations 12-15 may be used to calculate the transformation matrix; equally accurate results are obtained via either approach. The correlation coefficient r_{xyz} is a valid statistical measure of the accuracy of the transformation for only four or more N-localizers. For three N-localizers, this correlation coefficient equals 1.0 because three points determine the orientation of a plane in three-dimensional space.

Conclusions

This article presents a novel method for calculating the transformation matrix that transforms coordinates from the two-dimensional coordinate system of a tomographic image into the three-dimensional coordinate system of the stereotactic frame. This method applies to three or more N-localizers; when applied to more than three N-localizers, it provides a statistical measure of the accuracy of the transformation in terms of a correlation coefficient. Because nonlinearity of a tomographic image, such as may occur in an MR image, degrades the accuracy of the transformation, this correlation coefficient may indicate whether a particular MR image is sufficiently free of nonlinear distortion to qualify for MR-guidance of a stereotactic procedure.

Additional Information

Disclosures

Conflicts of interest: The authors have declared that no conflicts of interest exist.

Acknowledgements

The author would like to thank Barbara Pedrick of the Stanford University Department of Neurosurgery for assistance in obtaining hard-to-find journal articles.

References

1. Brown RA: A computerized tomography-computer graphics approach to stereotaxic localization. J Neurosurg. 1979, 50:715-20.
2. Brown RA: A stereotactic head frame for use with CT body scanners . Invest Radiol. 1979, 14:300-4.
3. Brown RA, Roberts TS: A stereotaxic frame and computer software for use with CT body scanners. Stereotactic Cerebral Irradiation, Proceedings of the INSERM Symposium on Stereotactic Irradiation. Szikla G (ed): Elsevier/North-Holland Biomedical Press, Amsterdam, the Netherlands; 1979. 25-27.
4. Brown RA, Roberts TS, Osborn AG: Stereotaxic frame and computer software for CT-directed neurosurgical localization. Invest Radiol. 1980, 15:308-12.
5. Perry JH, Rosenbaum AE, Lunsford LD, Swink CA, Zorub DS: Computed tomography/guided stereotactic surgery: Conception and development of a new stereotactic methodology. Neurosurg. 1980, 7:376-81.
6. Leksell L, Jernberg B: Stereotaxis and tomography. A technical note . Acta Neurochir (Wien). 1980, 52:1-7.
7. Brown RA, Roberts T, Osborn AG: Simplified CT-guided stereotaxic biopsy. AJNR Am J Neuroradiol. 1981, 2:181-4.
8. Goerss S, Kelly PJ, Kall B, Alker GJ Jr: A computed tomographic stereotactic adaptation system. Neurosurg. 1982, 10:375-9.
9. Dubois PJ, Nashold BS, Perry J, Burger P, Bowyer K, Heinz ER, Drayer BP, Bigner S, Higgins AC: CT-guided stereotaxis using a modified conventional stereotaxic frame . AJNR Am J Neuroradiol. 1982, 3:345-51.
10. Lunsford LD: A dedicated CT system for the stereotactic operating room . Appl Neurophysiol. 1982, 45:374-8.

11. Apuzzo ML, Sabshin JK: Computed tomographic guidance stereotaxis in the management of intracranial mass lesions. Neurosurg. 1983, 12:277-85.
12. Alker G, Kelly PJ, Kall B, Goerss S: Stereotaxic laser ablation of intracranial lesions. AJNR Am J Neuroradiol. 1983, 4:727-30.
13. Heilbrun MP, Roberts TS, Apuzzo ML, Wells TH Jr, Sabshin JK: Preliminary experience with Brown-Roberts-Wells (BRW) computerized tomography stereotaxic guidance system. J Neurosurg. 1983, 59:217-22.
14. Leksell L: Stereotactic radiosurgery. J Neurol Neurosurg Psychiatry. 1983, 46:797-803.
15. Thomas DG, Anderson RE, du Boulay GH: CT-guided stereotactic neurosurgery: Experience in 24 cases with a new stereotactic system. J Neurol Neurosurg Psychiatry. 1984, 47:9-16.
16. Bullard DE, Nashold BS Jr, Osborne D, Burger PC, Dubois P: CT-guided stereotactic biopsies using a modified frame and Gildenberg techniques. J Neurol Neurosurg Psychiatry. 1984, 47:590-5.
17. Apuzzo ML, Chandrasoma PT, Zelman V, Giannotta SL, Weiss MH: Computed tomographic guidance stereotaxis in the management of lesions of the third ventricular region. Neurosurg. 1984, 15:502-8.
18. Leksell L, Leksell D, Schwebel J: Stereotaxis and nuclear magnetic resonance. J Neurol Neurosurg Psychiatry. 1985, 48:14-8.
19. Thomas DG, Davis CH, Ingram S, Olney JS, Bydder GM, Young IR: Stereotaxic biopsy of the brain under MR imaging control. AJNR Am J Neuroradiol. 1986, 7:161-3.
20. Lunsford LD, Martinez AJ, Latchaw RE: Stereotaxic surgery with a magnetic resonance- and computerized tomography-compatible system. J Neurosurg. 1986, 64:872-8.
21. Heilbrun MP, Sunderland PM, McDonald PR, Wells TH Jr, Cosman E, Ganz E: Brown-Roberts-Wells stereotactic frame modifications to accomplish magnetic resonance imaging guidance in three planes. Appl Neurophysiol. 1987, 50:143-52.
22. Apuzzo ML, Petrovich Z, Luxton G, Jepson JH, Cohen D, Breeze RE: Interstitial radiobrachytherapy of malignant cerebral neoplasms: rationale, methodology, prospects. Neurol Res. 1987, 9:91-100.
23. Apuzzo ML, Chandrasoma PT, Cohen D, Zee CS, Zelman V: Computed imaging stereotaxy: Experience and perspective related to 500 procedures applied to brain masses. Neurosurg. 1987, 20:930-7.
24. Debaene A, Gomez A, Lavieille J, Alessandri C, Legre J: Stereotactic CT localization and biopsy of brain tumours using the Leksell frame. A study of 45 cases (article in English and French). J Neuroradiol. 1988, 15:266-75.
25. Loeffler JS, Alexander E 3rd, Siddon RL, Saunders WM, Coleman CN, Winston KR: Stereotactic radiosurgery for intracranial arteriovenous malformations using a standard linear accelerator. Int J Radiat Oncol Biol Phys. 1989 , 17:673-7.
26. Couldwell WT, Apuzzo ML: Initial experience related to the use of the Cosman-Roberts-Wells stereotactic instrument. Technical note. J Neurosurg. 1990, 72:145-8.
27. Lunsford LD, Coffey RJ, Cojocaru T, Leksell D: Image-guided stereotactic surgery: A 10-year evolutionary experience. Stereotact Funct Neurosurg. 1990, 54-55:375-87.
28. Andoh K, Nakamae H, Ohkoshi T, Odagiri K, Kyuma Y, Hayashi A: Technical note: Enhanced MR-guided stereotaxic brain surgery with the patient under general anesthesia. AJNR Am J Neuroradiol. 1991, 12:135-8.
29. Pell MF, Thomas DG: The initial experience with the Cosman-Roberts-Wells stereotactic system. Br J Neurosurg. 1991, 5:123-8.
30. Martínez R, Vaquero J: Image-directed functional neurosurgery with the Cosman-Roberts-Wells stereotactic instrument. Acta Neurochir (Wien). 1991, 113:176-9.
31. Pillay PK, Barnett G, Awad I: MRI-guided stereotactic placement of depth electrodes in temporal lobe epilepsy. Br J Neurosurg. 1992, 6:47-53.
32. Maciunas RJ, Kessler RM, Maurer C, Mandava V, Watt G, Smith G: Positron emission tomography imaging-directed stereotactic neurosurgery. Stereotact Funct Neurosurg. 1992, 58:134-40.
33. Kondziolka D, Dempsey PK, Lunsford LD, Kestle JR, Dolan EJ, Kanal E, Tasker RR: A comparison between magnetic resonance imaging and computed tomography for stereotactic coordinate determination. Neurosurg. 1992, 30:402-6.
34. Sofat A, Hughes S, Briggs J, Beaney RP, Thomas DG: Stereotactic brachytherapy for malignant glioma using a relocatable frame. Br J Neurosurg. 1992, 6:543-8.

35. Liang JA, Lin FJ, Tsai MD, Tu CP, Hsiao AC: Implementation of stereotactic focal radiotherapy for intracranial arteriovenous malformations using a linear accelerator. J Formos Med Assoc. 1993, 92:988-94.
36. Kratimenos GP, Thomas DG, Shorvon SD, Fish DR: Stereotactic insertion of intracerebral electrodes in the investigation of epilepsy. Br J Neurosurg. 1993, 7:45-52.
37. Pell MF, Thomas DG, Krateminos GP: Stereotactic management of intrinsic brain stem lesions. Ann Acad Med Singapore. 1993, 22:447-51.
38. Matsumoto K, Higashi H, Tomita S, Ohmoto T: Pineal region tumours treated with interstitial brachytherapy with low activity sources (192-iridium). Acta Neurochir (Wien). 1995, 136:21-8.
39. Dormont D, Cornu P, Pidoux B, Bonnet AM, Biondi A, Oppenheim C, Hasboun D, Damier P, Cuchet E, Philippon J, Agid Y, Marsault C: Chronic thalamic stimulation with three-dimensional MR stereotactic guidance. AJNR Am J Neuroradiol. 1997, 18:1093-107.
40. Levivier M, Massager N, Wikler D, Lorenzoni J, Ruiz S, Devriendt D, David P, Desmedt F, Simon S, Van Houtte P, Brotchi J, Goldman S: Use of stereotactic PET images in dosimetry planning of radiosurgery for brain tumors: clinical experience and proposed classification. J Nucl Med. 2004, 45:1146-54.
41. Lunsford LD, Niranjan A, Khan AA, Kondziolka D: Establishing a benchmark for complications using frame-based stereotactic surgery. Stereotact Funct Neurosurg. 2008, 86:278-87. 10.1159/000147636
42. Brown RA, Nelson JA: Invention of the N-localizer for stereotactic neurosurgery and its use in the Brown-Roberts-Wells stereotactic frame. Neurosurg. 2012, 70:173-6. 10.1227/NEU.0b013e318246a4f7
43. Brown RA, Nelson JA: The Origin of the N-Localizer for Stereotactic Neurosurgery . http://www.cureus.com. 2013, 5:e140. http://www.cureus.com/articles/2335-the-origin-of-the-n-localizer-for-stereotactic-neurosurgery.
44. Brown RA: The Mathematics of the N-Localizer for Stereotactic Neurosurgery . http://www.cureus.com. 2013, 5:e142. http://www.cureus.com/articles/2336-the-mathematics-of-the-n-localizer-for-stereotactic-neurosurgery.
45. Brown RA, Nelson JA: The History and Mathematics of the N-Localizer for Stereotactic Neurosurgery. http://www.cureus.com. 2014, 6:e156. http://www.cureus.com/articles/2391-the-history-and-mathematics-of-the-n-localizer-for-stereotactic-neurosurgery.
46. Thomas GB: Calculus and analytic geometry (3rd ed). Addison-Wesley Publishing Company, Inc., Reading, Massachusetts; 1966. 697-701.
47. Thomas GB: Calculus and analytic geometry (3rd ed). Addison-Wesley Publishing Company, Inc., Reading, Massachusetts; 1966. 419-425.
48. Spiegel MR: Schaum's Theory and Problems of Statistics (Schaum's Outline Series) . McGraw-Hill Book Company, New York; 1961. 255.
49. Spiegel MR: Schaum's Theory and Problems of Statistics (Schaum's Outline Series) . McGraw-Hill Book Company, New York; 1961. 271.